International Journal of ChemTech Research
CODEN (USA): IJCRGG ISSN: 0974-4290
Vol.7, No.3, pp 1399-1405, 2014-2015

ICONN 2015 [5th -7th Feb 2015]
International Conference on Nanoscience and Nanotechnology-2015
SRM University, Chennai, India

Correlating the optical absorption of nanostructured SnO_2:Au system with its gas sensing behavior

M. Sirisha[1], G. Veerabrahmachari[1], P. Manjula[1], T.S.S.Subramanian[2] and Sunkara V. Manorama[1]*

Nanomaterials Laboratory, Inorganic and Physical Chemistry Division CSIR-Indian Institute of Chemical Technology, Uppal Road, Tarnaka.Hyderabad-500 007
[2]Department of Electrical Engineering, Indian Institute of Technology (IIT) Delhi.

Abstract : SnO_2 is a well known wide band gap n-type semi-conducting material with tetragonal rutile type crystal structure. It has high sensitivity towards analyte gases and its sensitivity and selectivity can be improved with different additives. In the present study the gas sensing behavior of SnO_2 and SnO_2/Au nanostructured materials have been correlated with the corresponding optical properties. The UV absorption spectra of the system before and after exposure to ethanol vapours have been studied on nanostructured SnO_2 incorporated with Au nanoparticles. These results on synthesized nanostructures have been compared with commercially available materials. The role of Au as inferred from gas sensing is primarily catalytic and interestingly the corresponding Plasmon peak is also considerably altered implying its role in the sensing phenomenon. The results have been explained on the structure and morphology of the materials and conclusions supported by TEM, XRD, UV absorption and gas sensing characteristics.
Keywords: optical absorption, nanostructured SnO_2:Au system gas sensing behavior.

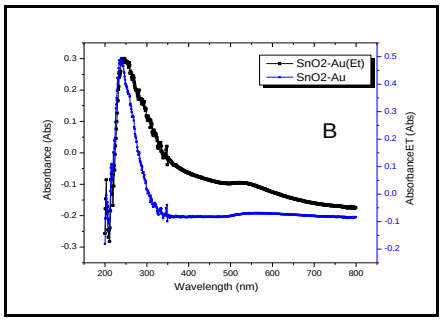

UV absorption spectra of SnO2/Au before and after ethanol exposure

Introduction:

The most important form of naturally occurring tin oxide (SnO_2) is cassiterite, with the tetragonal rutile-type crystalline structure. It is an n-type wide band gap semiconductor (Eg =3.6 eV at 300 K)[1-2] and presents an appropriate combination of chemical, electronic and optical properties that make it advantageous in various applications in catalysis[3], gas-sensing[4], anode materials for lithium-ion batteries[5], DSSCs[6], and so on. In particular, due to its stability, sensitivity, and low cost, more recently much attention has been focused on SnO_2 for potential use in environmental remediation[7-8]. In particular nanostructured SnO_2, is an interesting material whose properties could be significantly improved in comparison with its bulk benefiting from the nanometre size effects. Rightly promoted by this expectation, various nanostructures of SnO_2 such as nanoparticles[9], nanorods[10], nanowires[11], nanotubes[12], porous spheres[13], hollow nanostructures[14],have been synthesized. These nanostructures have displayed highly potent results for gas sensing and many other applications[15-19].

Factors Influencing the Sensor Efficiency:

Recent progress in micro- and nanotechnologies[20–24] have opened a corridor for new material platforms, miniaturized device fabrication, and novel sensing concepts for improving sensitivity, fast response time, long term stability and low power consumption of the next generation sensors[25], It is important to note that there are many factors that influence the efficiency of a sensor device. Primarily the particular sensor material defined by its chemistry, size and shape dependent properties like surface area[26], crystallinity[27], void space in particles[28], microstructure of material and the associated electronic properties play a key role in developing an efficient sensor[24, 29–34] Progress in sensors development requires a combination of skills in materials synthesis, understanding the chemical, physical, thermal and electronic properties of materials, as well as engineering of devices using various nano structured materials that exhibit significantly tunable size and morphology dependent chemical and physical properties[35].

Semiconducting Metal Oxide Sensors:

A wide range of materials have been reported to be used for the sensor fabrication such as metals, metal oxides[36,38,39], polymers[40], carbon nanomaterials[37], chalcogens and many other composite materials[40–42]. Among these, the most suitable are semiconducting metal oxides that have become very popular because of their simple and inexpensive synthesis procedures, high stability, easy to miniaturize, rugged, reliable, simplicity in the device fabrication and the possibility to operate over a range of conditions including high temperatures[43]. Metal oxides such as SnO_2, CuO[43], ZnO[44], Cr_2O_3[45], WO_3[46] and TiO_2[47-49], mainly because of their semiconducting nature, are used extensively for resistive type chemical gas sensing applications.

Introduction to material:

Tin Dioxide Sensors:

Among the many semiconducting gas sensors, tin oxide based gas sensors have undergone extensive research and development due to their high sensitivity towards analyte gases and the possibility of tailoring the material to sense several test gases like highly explosive hydrogen, methane, poisonous CO, NOx, SO_2, and volatile organic compounds. Tin dioxide semiconductor gas sensors were first proposed[50] and patented in 1962[51] and since then SnO_2 based sensors have become a leading choice for solid state gas detectors in industrial, commercial and domestic fields. Several review articles[36, 27, 52-54] were documented to cover the scientific literature on SnO_2 sensors including the works on the detailed discussion of proposed electronic mechanisms for sensor response by Yamazoe based on experimentally observed trends[55] The review by Park and Akbar[56] provides a comprehensive discussion on the basic principles involved at the gas-solid interface of the sensors. This review mainly emphasizes on the micro structural properties and their effect on the SnO_2 sensor function.

Even though the basic understanding of physiochemical properties of SnO_2 and how these properties related to sensor applications has been developed dramatically, improvement in sensor efficiency still depends on empirical studies. So there is a need for a careful analysis of micro structural properties and their correlation with sensor performance and from these studies, to establish direct links between microstructure and its sensor performance which is an important step towards achieving efficient sensors for specific sensor applications.

As sensing is the surface phenomena, increasing the surface area with change in microstructure of materials is an effective method to improve the sensitivity. Nanomaterials are ideal candidates that satisfy the

above criteria and exhibit exceptional chemical and physical properties like thermal stability, high surface area and large pore volume per unit mass that can be exploited for efficient sensor fabrication. In addition, these materials have been shown to require facile and 'green' synthetic procedures and display long-term stability and recyclability which is necessary for commercialization. As more and more types of ''smart'' nanomaterials with unique and tunable properties continue to be invented, increasing numbers of efficient and selective nanosensors are expected to emerge.

Experimental work:

In the present study SnO_2 nanospheres were used. The material was synthesized by Modified hydrothermal Method. In which 1g of Sodium stannate tri hydrate and 2g of glucose are dissolved in 30ml water. Temperature of 50°c is maintained for 12 hours. The solution is then allowed to cool till room temperature. It is then Centrifuged washed then dried at 60°c to evaporate water and organic material. The obtained material is crushed and the powder is obtained. This synthesis procedure has been described in detail in our earlier work[2].

Noble metal Au is doped with the synthesized SnO_2 by impregnation method using Gold chloride ($HAuCl_4.3H_2O$) and tri sodium citrate. Temperature of 70°C is maintained for 30 minutes. Later it is centrifuged and washed, dried and the powdered sample is collected. The same process is repeated for the commercially available SnO_2 also. The obtained Au incorporated SnO_2 samples are pelletized with KBr for UV-DRS. Ethanol vapours are collected by using syringe and needle and continuously pumped to the hot pellets. The samples are pre-heated at 200°C to stabilize the surface before exposure to ethanol vapours.

Results and discussions:

X-Ray Diffraction studies:

X-ray diffraction studies confirmed that the synthesized materials were SnO_2 of Cassiterite structure and all the diffraction peaks agree with the reported JCPDS data (Card No: 21-1250). Figure (1) shows the powder XRD patterns of the as-synthesized and samples annealed at varying temperatures in air. The as-synthesized sample (pattern a) shows broad peaks because of the low crystallinity and the average crystallite size calculated by applying the Scherrer's formula to the major diffraction peak is about 1.9 nm. The crystallite size is found to increase with increase in the annealing temperature as observed qualitatively by a narrowing of the diffraction peaks. The average crystallite size of the calcined sample is 7.2 nm, respectively.

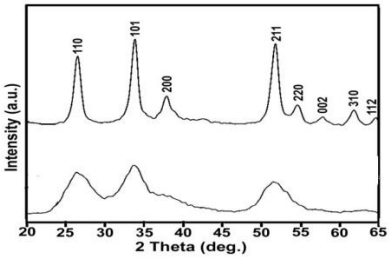

Figure1.XRD patterns of (a) as synthesized and (b) Annealed sample

TEM: Figure 2 shows the TEM image of synthesized SnO_2 incorporated with Au. It is seen that the average SnO_2 nanospheres have a size around 80-100nm. The micrograph reveals that the as synthesized product showing reasonably monodispersed nanospheres and the high-magnification TEM image (not shown) reveals that each nanosphere comprises of few hundred primary nanoparticles with a size of about 2-3 nm.

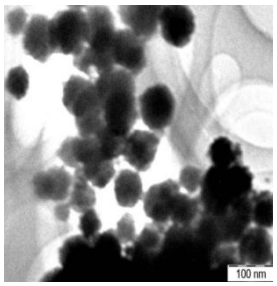

Figure 2: TEM image of Au incorporated SnO_2 nanospheres

Optical absorption studies on SnO_2/Au :

SnO_2 reveals a sharp optical absorption when the size is reduced to nanometre range. As seen from the UV-DRS (Figure 3) of the two samples one distinct feature is the sharp absorption of the nanosized spheres compared to the commercial SnO_2. The absorption edge is shifted to lower wavelength region which is indicative of an increase in the band gap. This is supportive of our claim that the nanosizing brings about a blue shift in the absorption edge. Conductivity is higher for (A) commercial SnO_2 compared to (B) synthesized SnO_2 this is because of the increased defects at the grain boundaries that contribute to the resistance. This is a very favourable situation as far as gas sensing is concerned for the simple reason that on exposure to the reducing gas the observed change in resistance is higher thereby contributing to the higher sensitivity values in the as synthesized materials when compared to the performance of commercial SnO_2.

UV-DRS studies on exposure to gas:

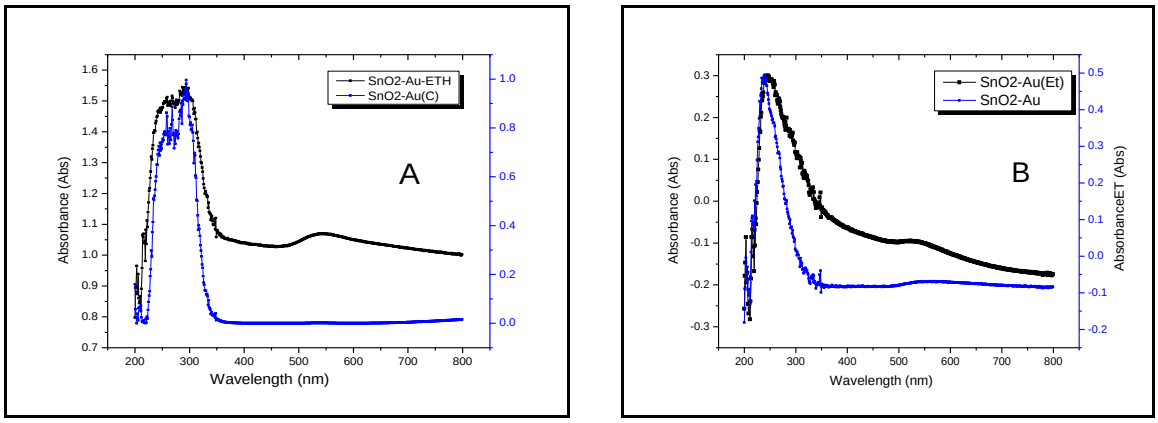

Figure 3: UV-DRS spectrum for commercial SnO_2/Au(A) and Synthesized SnO_2/Au (B) Before exposure (Blue colored) and after Ethanol exposure (Black colored)

Figure 3 shows the UV-DRS spectrum of commercial SnO_2 and SnO_2 nanospheres incorporated with 1.5 wt% Au. As seen in Figure when compared to spectrum of sample before ethanol exposure in the presence of heating there is a broadening of the absorption peak. This could be correlated to the creation of oxygen vacancies on the surface. This could be hypothesized on the following lines. The synthesized SnO_2 is semiconducting with general formula SnO_{2-X}. After ethanol exposure conductivity of synthesized SnO_2 increases and this increase is because of creation of additional oxygen vacancies[70]. These oxygen vacancies are represented with the broadening of the peak towards higher wavelength. Compared to the commercial SnO_2 sample the SnO_2 nanospheres synthesized exhibit a better sensor performance. The SnO_2 shows a broadening into the visible spectral region. implying a larger oxygen or active sites like O^{2-} etc that are amenable for sensor response. Another significant observation is the appearance of Au plasmon peak. The Au Plasmon peak is insignificant in the spectrum of the SnO2:Au before exposure to ethanol in both the samples. But on exposure to ethanol this peak appears. This observation could be correlated with role of Au in the sensing mechanism which in our earlier works was ttributed to its catalytic and surface work function modification.

Results and discussions:

Gas sensing characteristics:

Gas sensing studies were performed comparatively in order to examine and compare the performance of tin dioxide nanospheres with commercially available tin dioxide powder which proved beyond doubt that the gas sensing was well exhibited as anticipated by the nanospheres. The reasons attributed for this is firstly the particle size and secondly the presence of oxygen vacancies that are in found in higher concentrations on the synthesized materials. Further systematically studying the influence of Au doping, cross sensitivity to other interfering gases, response characteristics giving the rate of response, operating temperature and gas concentration study to estimate the minimum or limit up to which the material can sense the test gas. Increase in Au concentration from 0 to 1.5 wt% in SnO_2 improves the room temperature response and above Au 1.5 wt% concentration i.e. 2.0 wt% the response is seen to decrease. This could be attributed to the optimal dispersal of Au 1.5 wt% in the SnO_2 matrix. The decrease in response for Au 2.0 wt % could be due to several factors like agglomeration of Au nanoparticles or masking of the active SnO_2 surface with Au particles for higher Au concentrations etc. Hence 1.5 wt% Au/SnO_2 has been selected and explored for further gas sensing characteristics.

Correlating the UV DRS studies with the gas sensing studies:

Several researchers have pointed out that pre-treatment conditions have an important impact on the performance of a catalyst. Absorption of gases like CO, H_2S, ethanol vapours causes change in optical constants by change in absorption due to luminescence. The absorption coefficient is always wavelength dependent which is analyzed by the absorbed photons. 'Au' absorbs the 'OH' group showing a shift in the Plasmon peak. The UV-DRS spectrum of the Au/SnO_2 shows a Plasmon peak at 554.38 nm indicative of the presence of Au nanoparticles. Pure gold nanoparticles are expected to give a Plasmon peak at about 520 nm. The high dielectric constant of SnO_2 causes a red shift and hence the absorbed Plasmon peak of Au in Au/SnO_2 appears at 554 nm[57].

Our studies also establish a perfect correspondence in the sensing performance with the broadening of the SnO_2 absorption peak attributing and ambiguously establishing the role of oxygen species and oxygen vacancies in the gas sensing phenomena[71].

Conclusions:

The studies reported in this paper bring the following conclusions:

1. Tin dioxide in the form of nanosize particles shows a better sensing performance compared to commercial sample. This has been attributed to the small size and presence of oxygen vacancies that favour the sening mechanism.

2. Au nanoparticles are shown to enhance the sensitivity to ethanol over the other interfering gases imparting a selectivity characteristic for this composition.

3. Nanosized Au on the SnO2 surface is show to be highlighted in the presence of reducing gases contributing to the role of phenomena similar to surface enhancement leading to exploring this material for other applications.

4. Correlating the UV-DRS studies with the gas sensing studies establishes and confirms the role of oxygen vacancies in the sensing phenomena.

This study has revealed the UV-Vis absorption spectroscopy that could be exploited for further exploring gas sensing in semiconducting oxide materials.

This study can now be continued further and extended to study this multifunctional character to be exploited for several device applications.

References:

1. Huang, H., Lee, Y. C.; Tan, O. K.; Zhou, W.; Peng, N.; Zhang, Q. *Nanotechnology* 2009, *20*, 115501–115506.
2. Manjula, P.; Satyanarayana, L.; Swarnalatha, Y.; Manorama, S. V. *Sens. Actuators B Chem.* 2009, *138*, 28–34.
3. Wang, S.; Huang, J.; Zhao, Y.; Wang, S.; Wang, X.; Zhang, T.; Wu, S.; Zhang, S.; Huang, W. *J. Mol. Catal. A Chem.* 2006, *259*, 245–252.
4. Sun, P.; Zhao, W.; Cao, Y.; Guan, Y.; Sun, Y.; Lu, G. *CrystEngComm* 2011, *13*, 3718–3724.
5. Liu, J.; Li, Y.; Huang, X.; Ding, R.; Hu, Y.; Jiang, J.; Liao, L. *J. Mater. Chem.* 2009, *19*, 1859–1864.
6. Gubbala, S.; Russell, H. B.; Shah, H.; Deb, B.; Jasinski, J.; Rypkema, H.; Sunkara, M. K. *Energy Environ. Sci.* 2009, *2*, 1302–1309.
7. Manjula, P.; Arunkumar, S.; Manorama, S. V. *Sens. Actuators B Chem.* 2011, *152*, 168–175.
8. Manjula, P.; Boppella, R.; Manorama, S. V. *ACS Appl. Mater. Interfaces* 2012, *4*, 6252–6260.
9. Zhang, L.-S.; Jiang, L.-Y.; Yan, H.-J.; Wang, W. D.; Wang, W.; Song, W.-G.; Guo, Y.-G.; Wan, L.-J. *J. Mater. Chem.* 2010, *20*, 5462–5467.
10. Zhang, L.-S.; Jiang, L.-Y.; Yan, H.-J.; Wang, W. D.; Wang, W.; Song, W.-G.; Guo, Y.-G.; Wan, L.-J. *J. Mater. Chem.* 2010, *20*, 5462–5467.
11. Xi, G.; Ye, J. *Inorg. Chem.* 2010, *49*, 2302–9.
12. Xu, X.; Zhuang, J.; Wang, X. *J. Am. Chem. Soc.* 2008, *130*, 12527–12535.
13. Xu, X.; Liang, J.; Zhou, H.; Lv, D.; Liang, F.; Yang, Z.; Ding, S.; Yu, D. *J. Mater. Chem. A* 2013, *1*, 2995.
14. Zhang, J.; Liu, X.; Wu, S.; Xu, M.; Guo, X.; Wang, S. *J. Mater. Chem.* 2010, *20*, 6453–6459.
15. Wu, W.; Zhang, S.; Zhou, J.; Xiao, X.; Ren, F.; Jiang, C. *Chemistry* 2011, *17*, 9708–9719.
16. Wang, H.; Li, B.; Gao, J.; Tang, M.; Feng, H.; Li, J.; Guo, L. *CrystEngComm* 2012, *14*, 5177–5181.
17. Gyger, F.; bner, M.; Feldmann, C.; Barsan, N.; Weimar, U. *Chem. Mater.* 2010, *22*, 4821–4827.
18. Huang, H.; Lee, Y. C.; Tan, O. K.; Zhou, W.; Peng, N.; Zhang, Q. *Nanotechnol.* 2009, *20*, 115501–115506.
19. Comini, E.; Baratto, C.; Concina, I.; Faglia, G.; Falasconi, M.; Ferroni, M.; Galstyan, V.; Gobbi, E.; Ponzoni, A.; Vomiero, A.; Zappa, D.; Sberveglieri, V.; Sberveglieri, G. *Sens. Actuators B Chem.* 2013, *179*, 3–20.
20. Shen, G. *Recent Pat. Nanotechnol.* 2008, *2*, 160–168.
21. Korotcenkov, G.; Cho, B. K.; Gulina, L.; Tolstoy, V. *Sens. Actuators B Chem.* 2009, *138*, 610–616.
22. Zhang, T.; Liu, L.; Qi, Q.; Li, S.; Lu, G. *Sens. Actuators B Chem.* 2009, *139*, 287–291.
23. Sysoev, V. V; Goschnick, J.; Schneider, T.; Strelcov, E.; Kolmakov, A. *Nano Lett.* 2007, *7*, 3182–3188.
24. Yeow, S. C.; Ong, W. L.; Wong, a. S. W.; Ho, G. W. *Sens. Actuators B Chem.* 2009, *143*, 295–301.
25. Mehrabi Matin, B.; Mortazavi, Y.; Khodadadi, A. A.; Abbasi, A.; Anaraki Firooz, A. *Sens. Actuators B Chem.* 2010, *151*, 140–145.
26. Lee, J.-H. *Sens. Actuators B Chem.* 2009, *140*, 319–336.
27. Arshak, K.; Moore, E.; Lyons, G. M.; Harris, J.; Clifford, S. *Sens. Rev.* 2004, *24*, 181–198.
28. Xi, G.; Ye, J. *Inorg. Chem.* 2010, *49*, 2302–2309.
29. Ramgir, N. S.; Hwang, Y. K.; Jhung, S. H.; Kim, H.-K.; Hwang, J.-S.; Mulla, I. S.; Chang, J.-S. *Appl. Surf. Sci.* 2006, *252*, 4298–4305.
30. Shimizu, Y.; Jono, A.; Hyodo, T.; Egashira, M. *Sens. Actuators B Chem.* 2005, *108*, 56–61.
31. Vaishampayan, M. V.; Deshmukh, R. G.; Walke, P.; Mulla, I. S. *Mater. Chem. Phys.* 2008, *109*, 230–234.
32. Choi, J.-K.; Hwang, I.-S.; Kim, S.-J.; Park, J.-S.; Park, S.-S.; Jeong, U.; Kang, Y. C.; Lee, J.-H. *Sens. Actuators B Chem.* 2010, *150*, 191–199.
33. Xu, J.; Wang, D.; Qin, L.; Yu, W.; Pan, Q. *Sens. Actuators B Chem.* 2009, *137*, 490–495.
34. Asefa, T.; Duncan, C. T.; Sharma, K. K. *Analyst* 2009, *134*, 1980–1990.
35. Liu, J.; Meng, F.; Zhong, Y.; Liu, J.; Chen, G.; Wan, Y.; Qian, K.; Mouli T., S. *J. Mater. Res.* 2011, *25*, 1992–2000.
36. Sun, Y.-F.; Liu, S.-B.; Meng, F.-L.; Liu, J.-H. J.-Y.; Jin, Z.; Kong, L.-T. *Sensors (Basel).* 2012, *12*, 2610–2631.
37. Kauffman, D. R.; Star, A. *Angew. Chemie Int. ed.* 2008, *47*, 6550–6570.
38. Comini, E.; Baratto, C.; Concina, I.; Faglia, G.; Falasconi, M.; Ferroni, M.; Galstyan, V.; Gobbi, E.; Ponzoni, A.; Vomiero, A.; Zappa, D.; Sberveglieri, V.; Sberveglieri, G. *Sens. Actuators B Chem.* 2013, *179*, 3–20.
39. Shen, G. *Recent Pat. Nanotechnol.* 2008, *2*, 160–168.

40. Consales, M.; Crescitelli,; Penza, M.; Aversa, P.; Veneri, P. D.; Giordano, M.; Cusano, *Sens. Actuators B Chem.* 2009, *138*, 351–361.
41. Choi, U.-S.; Sakai, G.; Shimanoe, K.; Yamazoe, N. *Sens. Actuators B Chem.* 2005, *107*, 397–401.
42. Moon, W. J.; Yu, J. H.; Choi, G. M. 2002, *87*, 464–470.
43. Miller, T. A.; Bakrania, S. D.; Perez, C.; Wooldridge, M. S. *Functional nanomaterials*, 2006, pp. 1–24.
44. Liu, Y.; Koep, E.; Liu, M. *Chem. Mater* 2005, *17*, 3997–4000.
45. Qin, Y.; Zhang, F.; Chen, Y.; Zhou, Y.; Li, J.; Zhu, A.; Luo, Y.; Tian, Y.; Yang, J. *J. Phys. Chem. C* 2012, *116*, 11994–12000
46. Gupta, S. K.; Joshi, A.; Kaur, M. *J. Chem. Sci*. 2010, *122*, 57–62.
47. Miremadi, B. K.; Singh, R. C.; Chen, Z.; Roy Morrison, S.; Colbow, K. *Sensors Actuators B Chem.* 1994, *21*, 1–4.
48. Teoh, L. G.; Hung, I. M.; Shieh, J.; Lai, W. H.; Hon, M. H. *Electrochem. Solid-State Lett.* 2003, *6*, G108.
49. Chung, Y. K. and G. A. and A. R. and J. S. I. and U.-J. *Phys. Scr.* 2007, *2007*, 157
50. Tetsuro Seiyama , Akio Kato , Kiyoshi Fujiishi, M. N. *Anal. Chem.* 1962, *34*, 1502–1503.
51. Kousuke Ihokura, J. W. *The Stannic Oxide Gas SensorPrinciples and Applications*; CRC Press, Boca Raton, FL,, 1994.
52. Bierwagen, O.; Nagata, T.; White, M. E.; Tsai, M.-Y.; Speck, J. S. *J. Mater. Res.* 2012, *27*, 2232–2236.
53. Schweizer-berberich, N. B. M. *Fresenius J. Anal. Chem.* 1999, *365*, 287–304.
54. Review, T.; Weimar, U. *J. Phys. Condens. Matter* 2003, *15*, 813–839.
55. Yamazoe, N. *Sens. Actuators B Chem.* 1991, *5*, 7–19.
56. C. O. Park, S. A. A. *J. Mater. Sci.* 2003, *38*, 4611–4637.
57. Zeller MV, Grutsch PA, Fehlner TP(1973) In Org. Chem12:1431.
58. Maiti, A.; Rodriguez, A.; Law, M.; Kung, P.; Mckinney, J. R.; Yang, P. *Nano Lett.* 2003, *3*, 1025–1028.
59. Tricoli, A.; Righettoni, M.; Teleki, A. *Angew. Chem. Int. Ed.* 2010, *49*, 7632–7659.
60. Manjula, P.; Arunkumar, S.; Manorama, S. V. *Sens. Actuators B Chem.* 2011, *152*, 168–175.
61. Sunkara Manorama, G. S. D. and V. J. R. *Appl. Phys. Lett.* 1994, *64*, 3163–3165.
62. Wang, L.; Deng, J.; Fei, T.; Zhang, T. *Sens. Actuators B Chem.* 2012, *164,*, 90–95.
63. Wang, C.; Chu, X.; Wu, M. *Sens. Actuators B Chem.* 2006, *113*, 320–323.
64. Li, C. C.; Yin, X. M.; Li, Q. H.; Wang, T. H. *Cryst.Eng.Comm* 2011, *13*, 1557–1563.
65. Sun, P.; Zhao, W.; Cao, Y.; Guan, Y.; Sun, Y.; Lu, G. *Cryst.Eng.Comm* 2011, *13*, 3718–3724.
66. Wang, W.-W.; Zhu, Y.-J.; Yang, L.-X. *Adv. Funct. Mater.* 2007, *17*.
67. Morrison, S. R. *The Chemical Physics of Surfaces*; PLENUM PRESS· NEW YORK AND LONDON, 1977.
68. Barsan, N.; Weimar, U. *J. Electroceramics* 2001, *7*, 143–167.
69. Sysoev, V. V; Goschnick, J.; Schneider, T.; Strelcov, E.; Kolmakov, A. *Nano Lett.* 2007, *7*, 3182–3188.
70. Daniela Amalric Popescu, Jean-Marie Herrmann, Alain Ensuque and FrancÓ ois Bozon-Verduraz, Phys. Chem. Chem. Phys., 2001, 3, 2522È2530.
71. Tripti Shukla, *Journal of Sensor Technology*, 2012, 2, 102-108.

*****